RESULTS AND DISCUSSION (I)

Dissection of the Myosin VI Walking Mechanism

According to the lever arm theory, the step sizes of myosin molecular motors are predicted to be proportional to the length of their lever arms. In optical trapping experiments along with single molecule fluorescence experiments, a single myosin V molecule with its six light chains for example was shown to processively step hand-over-hand on actin filaments with a step size of 36 nm (Figure 26)[34,45,46].

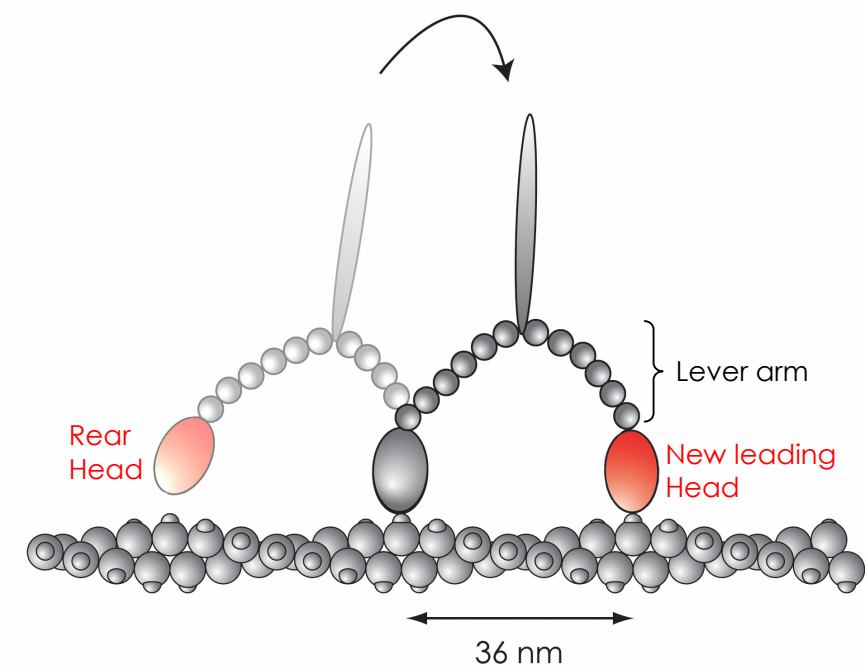

Figure 26: 36 nm displacement of the center of mass of a myosin V molecule as determined in optical trapping experiments. The molecule swings its rear head in front of the leading head and becomes the new leading head (shown in red). This mechanism is referred to as the hand over hand walking.

Myosin VI on the other hand has a short lever arm with only two light chains. Thus, myosin VI is expected to take ~10 nm non-processive steps according to the lever arm model (Figure 27).

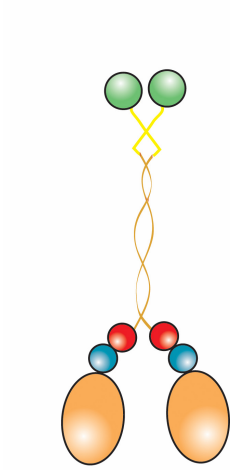

Figure 27: Schematic structure of the wild type myosin VI construct. The wild type head domain and the coiled coil domain that was truncated at Ala-990 are shown in orange. The unique insert bound calmodulin is colored blue and the IQ bound calmodulin is colored red. The yellow part represents the GCN4 coiled coil domain, followed by the YFP shown in green.

However, as myosin V, myosin VI was shown to walk processively on actin with a step size of 36 nm in single molecule optical trapping experiments[35]. Therefore, myosin VI has been argued to be the first exception to the widely established lever arm model. Thus, it was critical to demonstrate whether this motor walks hand-over-hand along actin in spite of its short lever arm that binds only two calmodulin light chains. The displacement of one head during one ATPase cycle can distinguish between putative walking mechanisms of a processive myosin VI dimer protein (Figure 39, Figure 40, and Figure 41). To follow one myosin VI head during its processive stepping on actin with nanometer resolution, a single molecule total internal reflection fluorescence (TIRF) microscopy assay was established (Figure 8).

Myosin VI Construct Design and Protein Expression

The N-terminus of the calmodulin light chains of the myosin VI protein was tagged with mutant cysteines that functioned as a unique site for specific fluorophore labeling. The specific and sub-stoichiometric labeling of one mutant calmodulin with a fluorophore allowed following the displacement of one myosin VI head in a single molecule TIRF microscopy assay.

A myosin VI dimer protein contains 44 wild type cysteines. Consequently, specific labeling of a mutant cysteine would require the deletion of 44 cysteines which would presumably lead to an unfunctional protein. To circumvent this problem, the calmodulin light chains in the myosin VI protein were N-terminally tagged with a KKCK or CCRECC motif to introduce cysteines that can specifically be labeled in the presence of 44 wild type cysteines. The KKCK motif enables a specific labeling of the mutant cysteine because the basic lysine residues presumably decrease locally the pKa of the embedded mutant cysteine and therefore make it more nucleophilic compared to the wild type cysteines. The CCRECC motif requires a tetra-functional dye for labeling that has four reactive sites (Figure 69). Because it is an extremely rare motif the dye only labels the CCRECC site.

The p2Bac/pFastBac-*wt*-CaM plasmid encoding the wild type calmodulin protein was used to create a calmodulin light chain that was N-terminally tagged with mutant cysteines for site specific fluorophore labeling. The restriction digested wild type myosin VI gene from the p2Bac/pFastBac-*wt*-M6-*wt*-CaM plasmid was then cloned into the p2Bac/pFastBac-*KKCK*-CaM^m or p2Bac/pFastBac-*CCRECC*-CaM^m plasmid containing the mutant calmodulin gene (Figure 28). The resulting p2Bac/pFastBac-M6-*KKCK*-CaM^m and p2Bac/pFastBac-M6-*CCRECC*-CaM^m dual expression plasmids coding for two different proteins were used for the protein expression in Sf9 cells.

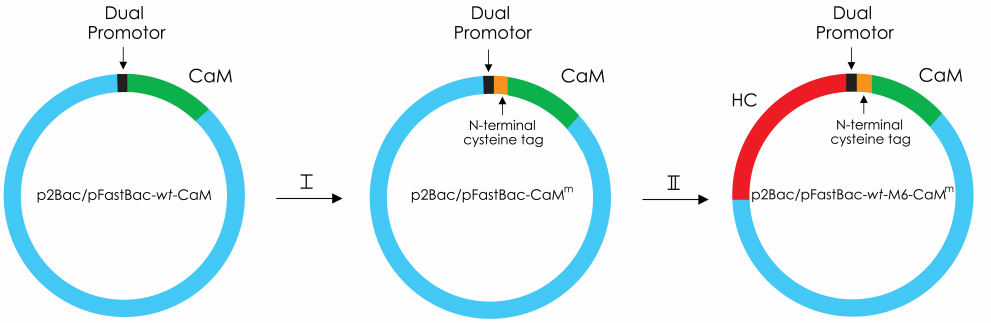

Figure 28: Construction of the p2Bac/pFastBac-*wt*-M6-CaM^m plasmid. First, the wild type calmodulin gene was PCR amplified from the p2Bac/pFastBac-*wt*-CaM plasmid using DNA primers that contained the KKCK- or CCRECC-tag (green) and reinserted into the p2Bac/pFastBac plasmid to give p2Bac/pFastBac-CaM^m plasmid (step I). Next, the YFP tagged wild type myosin VI heavy chain (red) was inserted into the p2Bac/pFastBac-CaM^m plasmid to give p2Bac/pFastBac-M6-*KKCK*-CaM^m plasmid (step II).

Insertion of the KKCK- and the CCRECC-tags into the wild type Calmodulin

The PCR amplification of the KKCK- and the CCRECC-tagged calmodulin genes from the p2Bac/pFastBac-*wt*-CaM plasmid resulted in a 500 bp and a 539 bp product, respectively. The PCR product was inserted back into the p2Bac/pFastBac plasmid and the insertion was verified by restriction digest analysis. The clones were DNA sequenced to ensure that the genes had the desired insertions and did not have any secondary mutations. The wild type myosin VI heavy chain gene was cloned into the p2Bac/pFastBac-CaM^{m} plasmid containing the desired calmodulin mutations. The correct insertion was verified by restriction digest analysis. Figure 29 shows an example of the involved cloning steps.

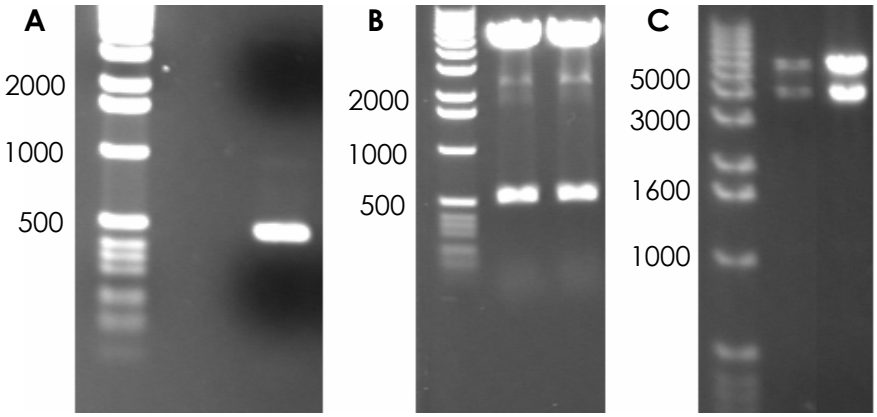

Figure 29: (A) PCR amplification of the N-terminally KKCK-tagged calmodulin DNA sequence from the p2Bac/pfastBac-*wt*-CaM plasmid template. **(B)** Restriction digest analysis of p2Bac/pfastBac-*wt*-CaM plasmid with Sal I and Not I restriction enzymes as a positive control (left lane). Restriction digest analysis to confirm the KKCK-tagged calmodulin gene insertion into the p2Bac/pfastBac using Sal I and Not I restriction enzymes (right lane). **(C)** Restriction digest analysis of p2Bac/pfastBac-*wt*-M6-*wt*-CaM plasmid EcoR I and BamH I restriction enzymes as a positive control (left lane). Restriction digest analysis to confirm the myosin VI heavy chain gene insertion into the p2Bac/pfastBac-*KKCK*-CaM^{m} plasmid using EcoR I and BamH I restriction enzymes (right lane).

Generation of the Recombinant Bacmid Plasmid

For the protein expression in the Sf9 cells, the p2Bac/pFastBac-M6-CC*RE*CC-CaM^{m} and the p2Bac/pFastBac-*wt*-M6-*KKCK*-CaM^{m} plasmids were transposed into the baculovirus shuttle vector (bacmid) in the DH10Bac™ *E. coli* cells. The recombination of the transfer vector p2Bac/pFastBac-M6-CC*RE*CC-CaM^{m} and p2Bac/pFastBac-*wt*-M6-*KKCK*-CaM^{m} with the bacmid is achieved by a site specific transposition. The successful recombination was confirmed by PCR analysis. An example of the PCR analysis is shown in Figure 30.

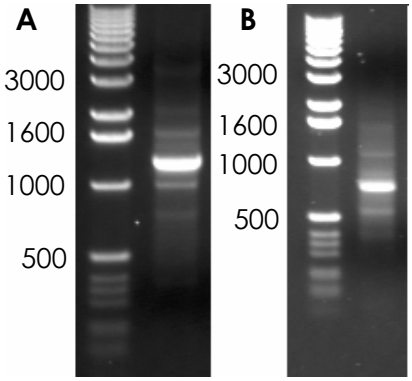

Figure 30: (A) PCR analysis of p2Bac/pfastBac-*KKCK*-CaM^{m} bacmid plasmid containing the myosin VI heavy chain and the N-terminally KKCK-tagged calmodulin gene sequences using the pGFP#4 / M13rev primer pair. The theoretically expected size of the PCR product is 1347 bp. **(B)** PCR analysis of p2Bac/pfastBac-*KKCK*-CaM^{m} bacmid plasmid containing the myosin VI heavy chain gene sequence and the N-terminally KKCK-tagged calmodulin gene sequence using the GenR#1 / M13fwd primer pair. The theoretically expected size of the PCR product is 608 bp.

Viral Titre Assays

The viral titre of the CCRECC-tagged myosin VI construct was determined to ensure that the bacmid plasmids were capable of infecting the Sf9 cells for high yield protein expression. The fluorescence of the YFP moiety in the CCRECC-tagged myosin VI construct was exploited to determine the titre of the amplified virus generations P_0 and P_1 in a 96-well plate format (Figure 21, Figure 22). The viral titre of the P_0 generation was determined to be 1.8×10^8 pfu/ml and of the P_1 generation 4.2×10^8 pfu/ml, respectively.

FLAG-tagged Protein Purification of the CCRECC- and KKCK-tagged Myosin VI Constructs

All myosin VI constructs contain a C-terminal FLAG tag and their first purification step therefore involved an affinity chromatography using anti-FLAG resin (Figure 31). After the batch elution, some FLAG-tagged YFP proteolytic degradation products were still present. The dye labeling of the KKCK-tagged and the CCRECC-tagged myosin VI constructs followed immediately after the batch elution from the Anti FLAG column.

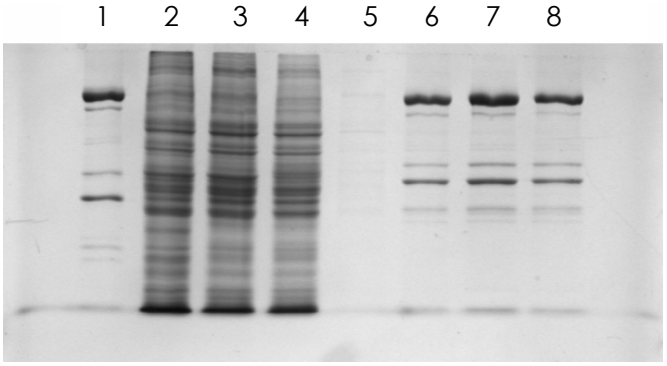

Figure 31: FLAG tagged batch protein purification of the KKCK-tagged myosin VI construct. Lane 1: Wild type myosin VI control, Lane 2: Cell lysate, Lane 3: Supernatant (SN), Lane 4: Flow-through (FT), Lane 5: Column wash, Lanes 6 - 8: Batch elution (10% SDS-polyacrylamide gel).

Protein Purification of the KKCK-tagged and the wild type Myosin VI constructs via Ion Exchange Chromatography

To remove excess Cy5 dye after the labeling reaction (Figure 72) and to further purify the protein from the YFP degradation products, the KKCK-tagged myosin VI construct was purified by cation exchange chromatography (MonoS) or anion exchange chromatography (MonoQ).

As opposed to MonoQ, the MonoS was capable of removing the proteolytic YFP degradation products (Figure 32, Figure 33). The wild type myosin VI construct was purified and labeled along with the KKCK-tagged construct as a negative control for labeling. The particular protein batch shown in Figure 33 was used throughout for all single molecule TIRF experiments.

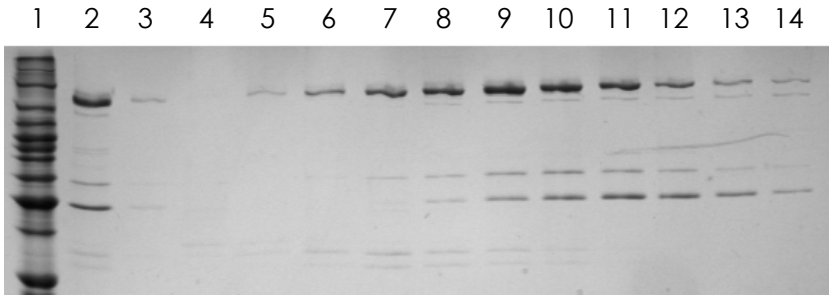

Figure 32: Anion exchange chromatography of the KKCK-tagged myosin VI protein using the MonoQ column (FPLC). The YFP proteolytic degradation products remaining from the FLAG-tagged batch purification could not be removed with the MonoQ column. Lane 1: Marker, Lane 2: Column load, Lane 3: FT, Lanes 4 - 14: Eluted fractions (10% SDS-polyacryl-amide gel).

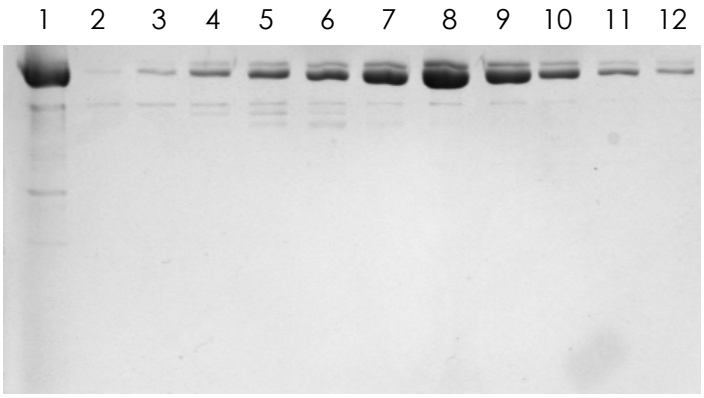

Figure 33: Cation exchange chromatography KKCK-tagged myosin VI protein purification using the MonoS column (FPLC). Lane 1: Wild type myosin VI as a size reference, Lanes 2-12: Eluted fractions from the MonoS column (10% SDS-polyacrylamide gel).

ReAsH Labeling of the CCRECC-tagged Myosin VI Construct

The CCRECC-tagged myosin VI construct was labeled with the ReAsH dye (a kind gift from Roger Tsien, UCSD)[73]. The ReAsH labeling of the CCRECC motif was virtually 100% specific (Figure 34). The excess dye was quantitatively removed by an over night incubation using Bio-Beads.

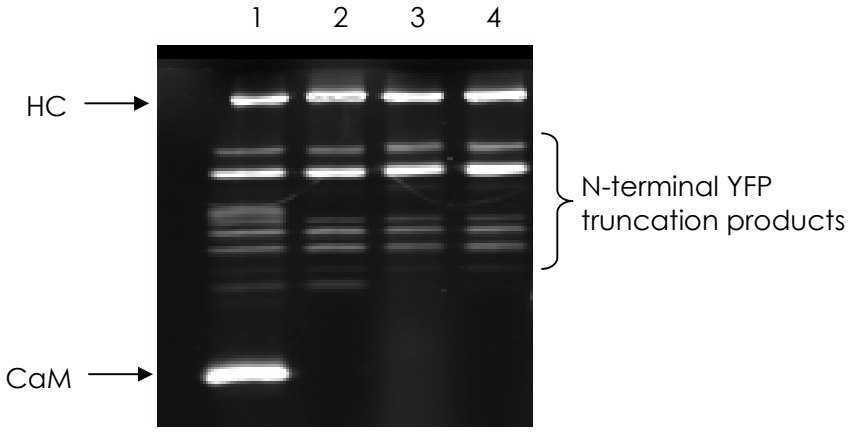

Figure 34: Analysis of the ReAsH labeling reaction via fluorescent scan of the SDS-polyacrylamide gel. The upper bands correspond to the interfering fluorescence of the YFP truncation products. Boiling the samples prior to electrophoresis resulted in complete loss of the YFP fluorescence in all samples due to YFP denaturation (not shown). Lane 1: CCRECC-tagged construct labeled with ReAsH, Lane 2: CCRECC-tagged construct labeled without ReAsH, Lane 3: wild type myosin VI labeled with ReAsH, Lane 4: wild type myosin VI labeled without ReAsH (2 mM EGTA, 15% SDS-polyacrylaminde gel).

EGTA SDS-PAGE gel revealed two bands of the N-terminally CCRECC-tagged calmodulin in a (1:1) ratio (Figure 35). Furthermore, selectively the upper protein band was labeled with the ReAsH dye. The N- and C-terminus of the unique insert bound calmodulin has been shown to interact tightly with the myosin VI heavy chain. Even in the presence of >100 µM calcium the calmodulins are bound to the unique insert in a permanent manner[48]. Therefore, the unique insert bound calmodulins were proposed to function as a structural element rather than a calcium dependent regulatory domain. It is therefore possible that N-terminally tagged calmodulin has reduced affinity to the unique insert due to its N-terminal alteration and as a result endogenously expressed calmodulin, which only differs at a single position from the *Drosophila* calmodulin can effectively competed with the mutant calmodulin for unique insert binding site.

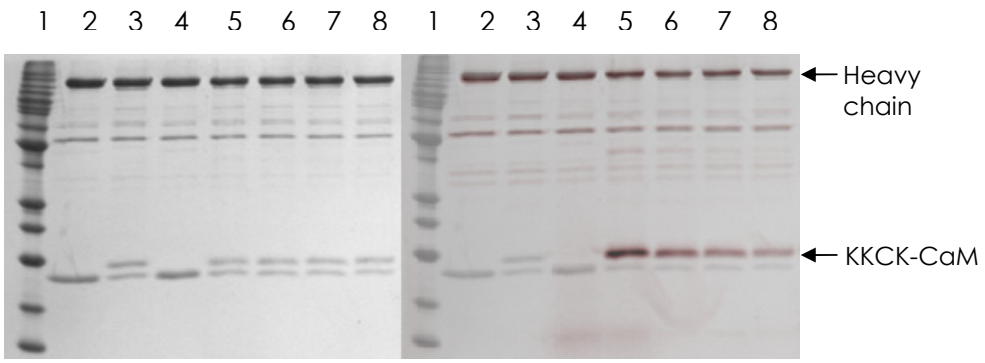

Figure 35: (Left) Coomassie stained SDS-polyacrylamide gel. Lane 1: Molecular marker, Lane 2: wild type myosin VI, Lane 3: CCRECC-tagged myosin VI, Lane 4: wild type myosin VI + ReAsH dye, Lane 5 - 8: CCRECC-tagged myosin VI + decreasing amount of ReAsH dye (2mM EGTA, 15% SDS-polyacrylamide gel). **(Right)** Fluorescent scan of the same SDS-poly-acrylamide gel. The fluorescent bands were colored red and superimposed with the coomassie bands. The calmodulin bands split in a (1:1) ratio in the CCRECC-tagged myosin VI containing band. The ReAsH dye specifically labeled the upper bands (arrow).

However, the fluorescent life time of the ReAsH dye was not sufficient for single molecule experiments as determined by photobleaching assays (Figure 36).

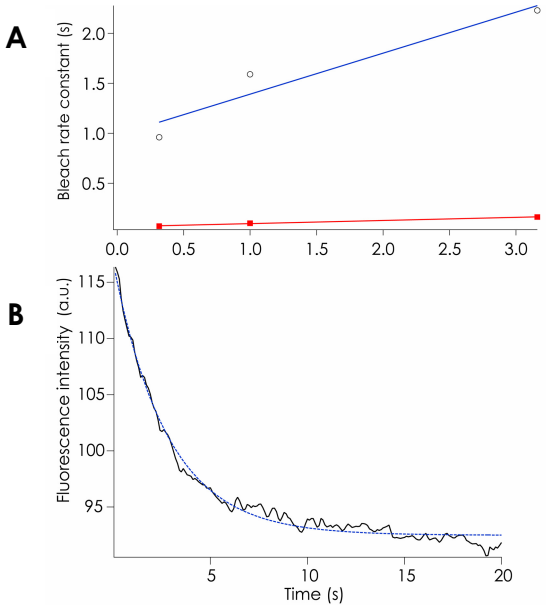

Figure 36: (**A**) Comparison of the photobleaching rates of the Cy3 dye that is commonly used in single molecule fluorescence experiments and the ReAsH dye. The ReAsH dye photobleaches 5 - 50 times faster than the Cy3 dye at comparable laser intensities which makes the ReAsH dye unsuitable for single molecule fluorescence assays. (**B**) Example photobleaching curve of the ReAsH dye.

Cy5 dye Labeling of the KKCK-tagged Myosin VI Construct

The fluorescent label was attached to an engineered cysteine that was inserted into the wild type cysteine-free calmodulin light chain of myosin VI. To attain labeling specificity over the 44 wild type cysteines in one myosin VI dimer, the calmodulin light chain was N-terminally tagged with lysine-lysine-cysteine-lysine (KKCK) and co-expressed with the myosin VI heavy chain in Sf9 cells. The high pKa of the lysines makes the mutant cysteine presumably more nucleophilic and therefore more reactive compared to the wild type cysteines, allowing specificity for the labeling reaction.

The labeling was >90% specific, as judged by the ratio of the heavy chain fluorescence to the light chain fluorescence in a fluorescence scan of an SDS-polyacrylamide gel (Figure 37).

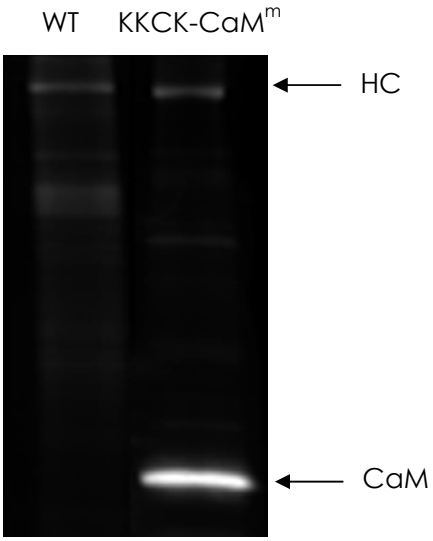

Figure 37: Analysis of the Cy5 labeling reaction via fluorescent scan of the SDS-polyacrylamide gel. The wild type myosin VI was labeled as a negative control (left). The wild type calmodulin in myosin VI is cysteine free, resulting in only the background labeling of the heavy chain with Cy5. The calmodulin band of the KKCK-tagged myosin VI protein showed extensive labeling with Cy5 (right). The Cy5 labeling of the calmodulin was >90% specificity as determined by the fluorescence ratio of the calmodulin band to the heavy chain band (2 mM EGTA, 15% SDS-polyacrylamide gel).

The KKCK-tagged protein was reacted with Cy5 with a (1:1) molar ratio of Cy5 dye to myosin VI dimer. At this molar ratio 10 - 15% of available binding sides were reacted with Cy5 dye as determined in titration experiment in which constant amount of protein was incubated with increasing amounts of Cy5 dye (Figure 38).

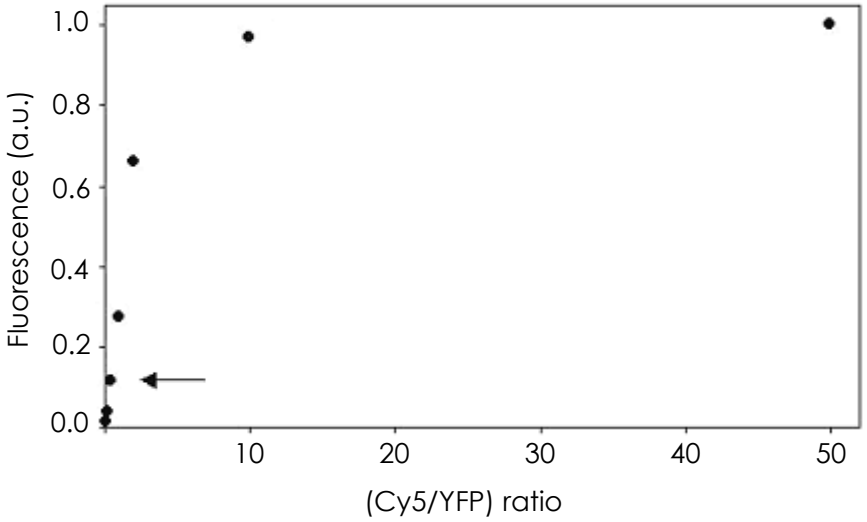

Figure 38: Titration curve of the KKCK-tagged myosin VI with increasing amounts of Cy5 dye. A (1:1) ratio of Cy5 dye to myosin VI dimer resulted in ~10 - 15% labeling (arrow).

In Vitro motility of the N-terminally tagged myosin VI constructs

Myosin VI expressed together with the N-terminally tagged calmodulins exhibited very similar properties in *in vitro* motility assays compared to the wild type myosin VI protein (Table 2).

Table 2: *In vitro* motility data of the myosin VI constructs

	WT-CaM Myosin VI	**CCRECC-CaM Myosin VI**	**KKCK-CaM Myosin VI**
Velocity (nm/s)	150 ± 40	230 ± 25	150 ±30

Possible Stepping Models of Myosin VI

Myosin VI was shown to walk processively on the actin filaments with a step size of 36 nm[35]. However, according to the lever arm model, with only two light chain domains the myosin VI step size was predicted to be ~10 nm. To span the 36 nm distance on actin, myosin VI must utilize some mechanically extensible elements to reach the observed distance. This putative element can in principle be N-terminal or C-terminal to the calmodulin light chain binding domain. If myosin VI walks hand-over-hand, the displacement of one head makes different and testable predictions in a single molecule TIRF experiment (Figure 39, Figure 40).

To elucidate the myosin VI stepping mechanism, fluorescently labeled single molecules of myosin VI walking on actin filaments were probed with nanometer resolution. If only one neck of myosin VI is dye labeled, the observed dye movement can distinguish between the proposed stepping mechanisms. According to a hand-over-hand model, the heads swap orientation during the stepping cycles resulting in an alternation of the leading positions. After each ATP hydrolysis the trailing head becomes the new leading head (Figure 39). The following figures illustrate possible stepping models of a myosin VI molecule labeled with a single fluorophore on one calmodulin, indicated in red.

In Figure 39, the putative mechanically extensible element was placed C-terminal to the labeled calmodulin. The first ~80 residues of the tail domain in the myosin VI dimer were shown to have a low propensity to form a coiled-coil[50,74]. Thus, this so called proximal tail domain is an attractive candidate for the putative extensible mechanical domain. In this model, a ~72 nm displacement of the fluorophore per ATPase cycle would be expected.

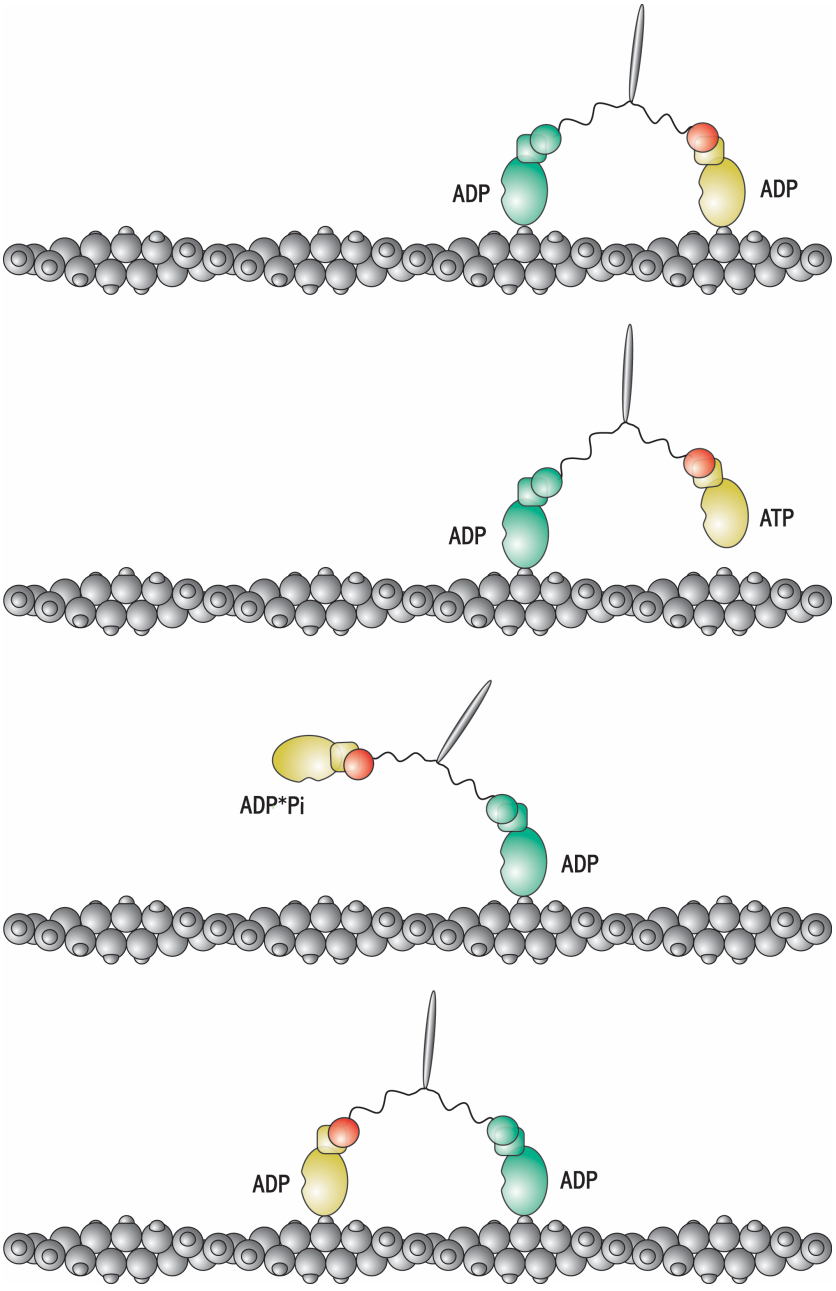

Figure 39: Possible hand-over-hand walking mechanism of myosin VI. The panel shows myosin VI walking to the left with its putative mechanically extensible element C-terminal to the labeled calmodulin light chain. A fluorescent label attached to one calmodulin (red) moves ~72 nm associated with each ATP hydrolysis. As a result, the trailing head (yellow) becomes the new leading head (green). The next step does not alter the fluorophore position and results in 0 nm displacement.

In Figure 40 the putative mechanically extensible element is N-terminal to the labeled calmodulin. In this model the displacement of one head always results in a ~36 nm displacement of the fluorophore.

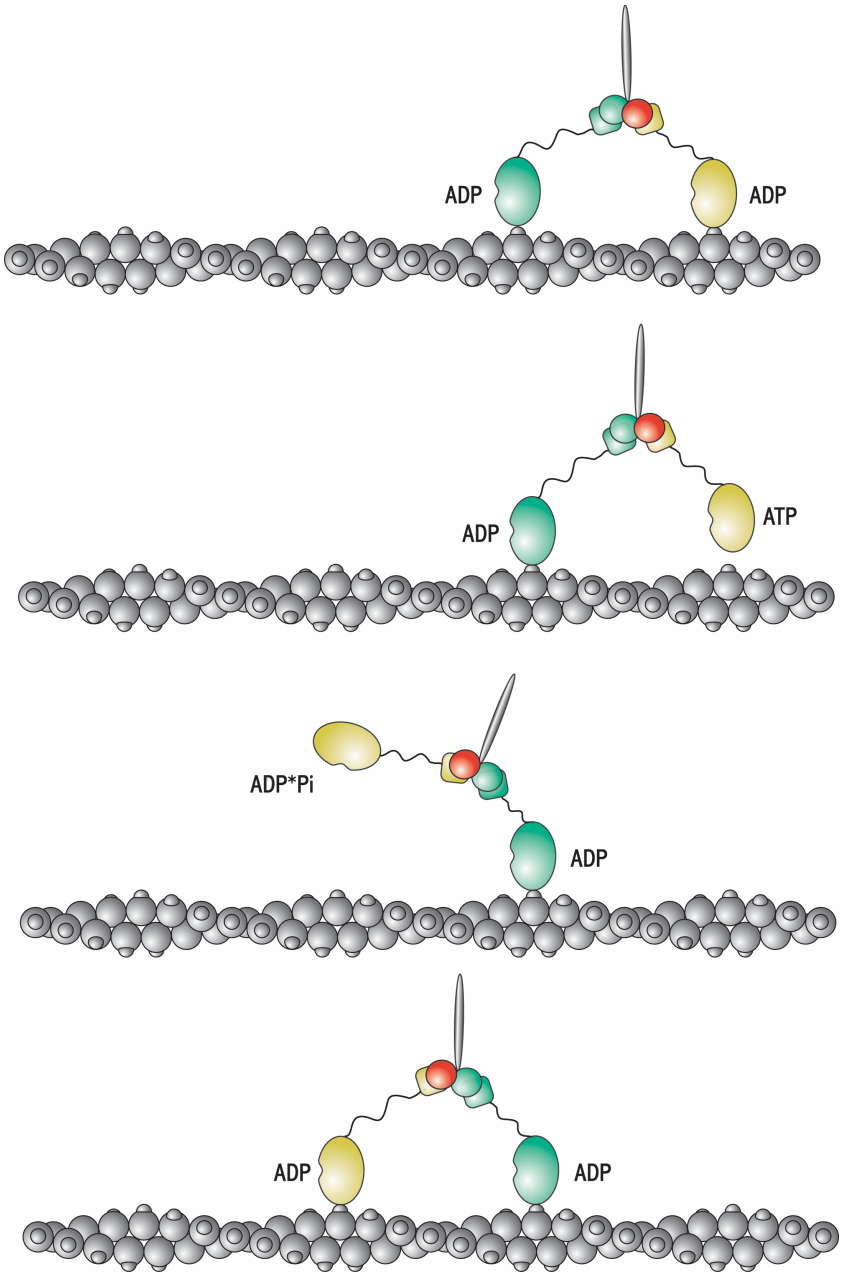

Figure 40: The panel shows a myosin VI molecule walking to the left with its putative mechanically extensible element positioned N-terminal to the labeled calmodulin. In this model, with each ATP hydrolysis the fluorescent label on calmodulin (red) is displaced ~36 nm.

An alternative to hand-over-hand walking is the inchworm model, which involves one head always serving as the leading head with the trailing head being pulled up from behind with each step (Figure 41). In this model the fluorophore displacement would result in ~36 nm regardless of where the putative mechanically extensible element is located.

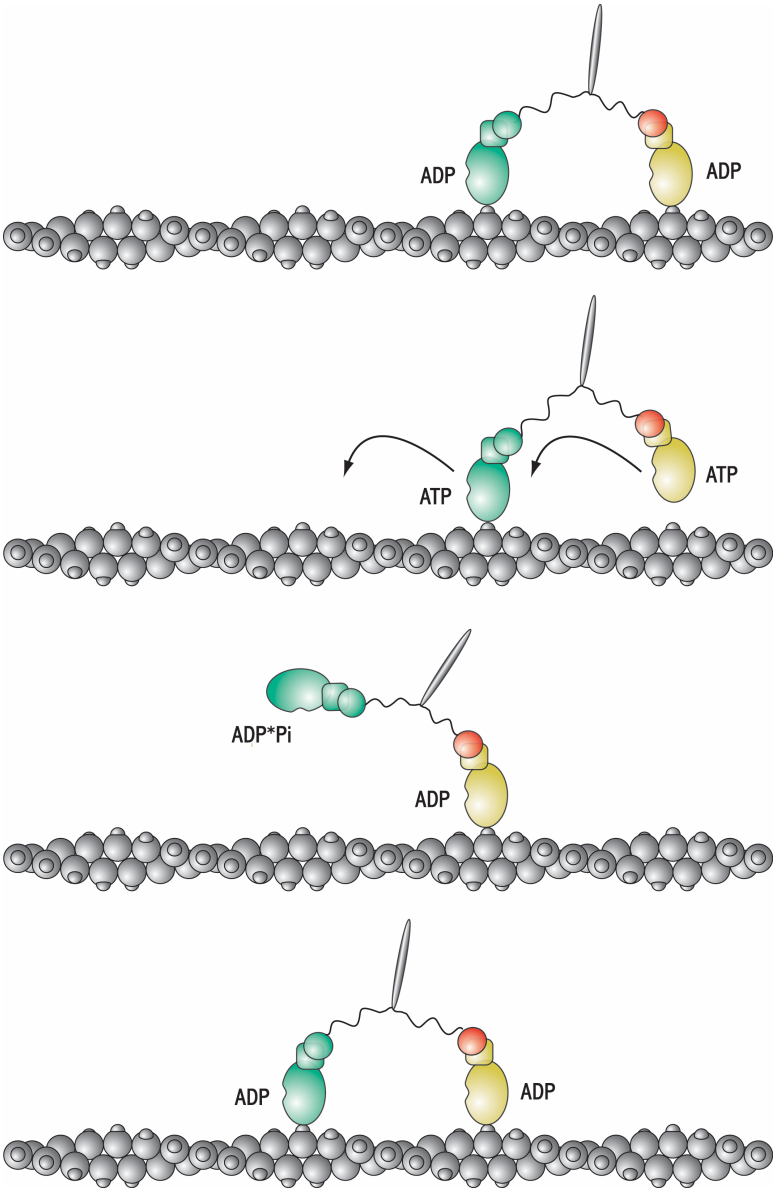

Figure 41: The panel shows a myosin VI molecule walking according to the inchworm model. The fluorophore moves ~36 nm with each ATP hydrolysis regardless where the putative mechanically extensible element is located.

Myosin VI Walks on Suspended Actin Filaments

Myosin VI has been shown to be processive in single molecule dual bead assays[35]. However, its processivity significantly decreased on entirely surface attached actin filaments presumably due to protein-surface interactions. To minimize surface interactions and thus to increase the myosin VI processivity, the actin filaments were elevated off the surface by either using nanometer

beads (Figure 43) or myosin S1 heads that were arrested in the rigor state with actin (Figure 42). The full-length myosin II molecules were reacted with N-Ethylmaleimide (NEM) to prevent the myosin heads from undergoing catalytic ATPase cycles. Myosin molecules arrested in the rigor state were non-specifically attached to the surface and subsequently bound to actin filaments. The myosin S1 head is 165 Å long, 65 Å wide and 45 Å thick. Thus, an actin filament stretched between surface-attached myosin S1 heads will be elevated from the surface (Figure 42).

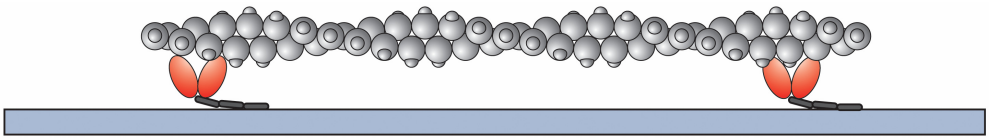

Figure 42: Illustration of the NEM treated full-length myosin II bound in rigor to the actin filaments. To prepare the flow cell, the cover slip was sparsely coated with the NEM bound rabbit skeletal myosin II filaments and actin was flown in to bind the myosin heads in rigor.

However, the preparation of these filaments was time consuming. A faster and more reproducible way to suspend the actin filaments proved to be the 90 nm bead assay (Figure 43). Actin filaments were suspended in solution by draping them between streptavidin coated spherical beads with 90 nm in diameter that sparsely coated the cover slip. The actin filaments were biotin labeled, which allowed them to adhere firmly to the streptavidin coated spherical beads. This geometry provided for long stretches of actin that were raised off the surface of the slide but were still for the most part within the total internal reflection excitation zone of the microscope.

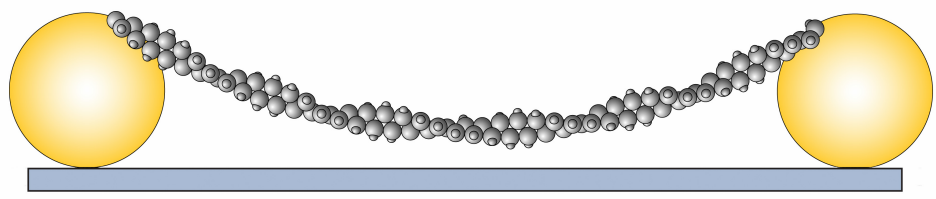

Figure 43: Illustration of biotinylated actin filaments that were stretched between 90 nm streptavidin coated beads. The filaments were elevated off the surface allowing the myosin VI proteins to walk processively on the actin filaments.

Processive walking of the fluorescently labeled myosin VI molecules on actin filaments was visualized as follows. The TRITC phalloidin actin filaments (excitation 557 nm, emission 576 nm) and the Cy5 (Absorption 649 nm, emission 670 nm) labeled myosin VI molecules were imaged in separate channels. Superimposing the images ensured that moving myosin VI spots were indeed associated with the actin filaments (Figure 44).

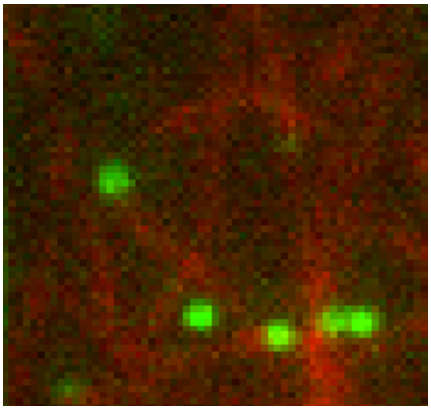

Figure 44: Superimposed images of TRITC labeled actin filaments (red) and the Cy5 labeled, single myosin VI molecules (green).

Myosin VI was found to walk processively on suspended actin filaments that were elevated off the surface which was sparsely coated with 90 nm beads. The average run length was 280 nm (n = 43) and run lengths up to 2.4 µm were observed (Figure 45). These measured run lengths are likely an underestimate because the protein can walk in or out of the evanescent field or the dye can photobleach while the myosin still walks along the actin filament.

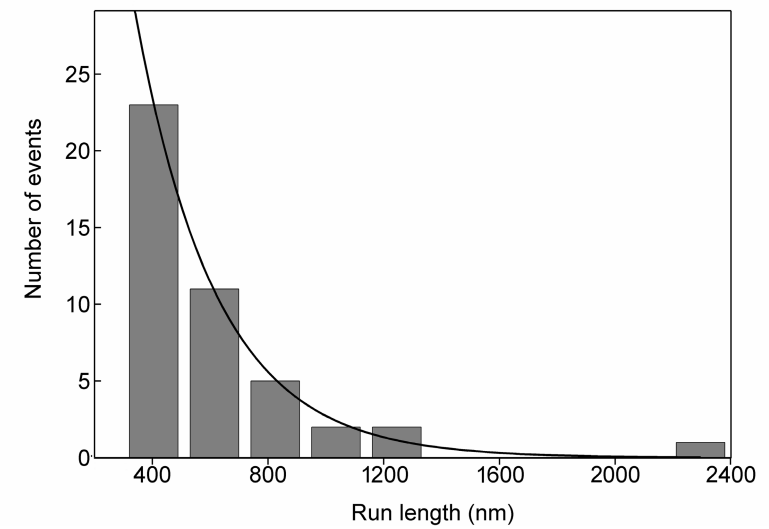

Figure 45: Run length distribution of single fluorescently labeled myosin VI molecules in the single molecule assays. Myosin VI walked processively on the suspended actin filaments with an average run length of 280 nm (n = 43). Run lengths ≥300 nm were tabulated and fit to a single exponential.

The suspended actin filaments were far enough from the surface to support long run lengths, but motors on these filaments appeared dim and were not generally suitable for a precise step size determination. Only molecules that were close to the surface were suitable for the step size determination, because only those provided quantum yields high enough was crucial for the accurate step size analysis as discussed in the following chapter.

Fluorophores were localized with Nanometer Resolution

Distinguishing between the predicted displacements of 72 nm vs. 36 nm of one labeled myosin VI head requires nanometer resolution. However, the resolution power of the conventional light microscopy methods for visible light of a single point source is limited to ~250 nm as defined by the Rayleigh criterion. Thus, following the diffraction limited image of one fluorophore with a ~250 nm diameter cannot distinguish between a 72 nm and 36 nm step (Figure 46).

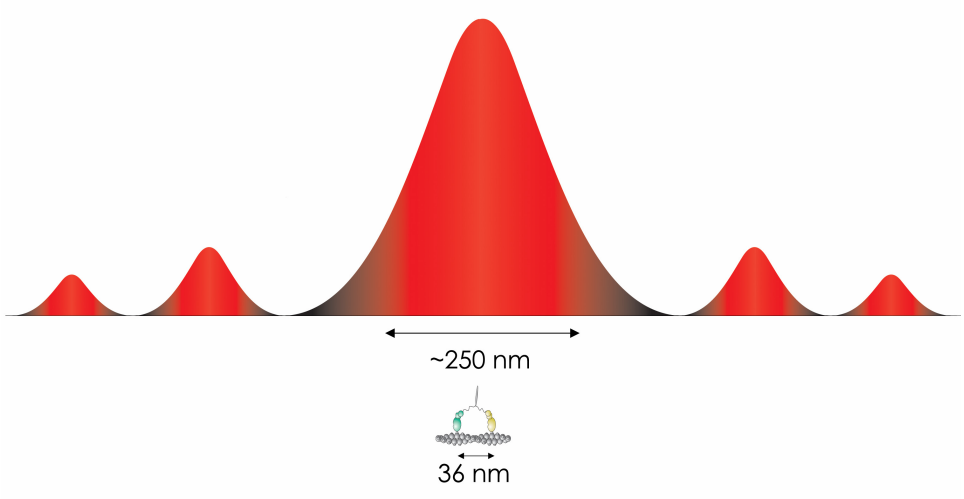

Figure 46: Diffraction limited image of a single fluorophore for visible light is approximately 250 nm. A 72 nm step size cannot be distinguished from a 36 nm step size by following the diffraction limited image of the emitted photons from a single fluorophore (proportions are to scale).

However, the center of the dyes can be determined with an arbitrarily high precision by collecting a sufficient number of photons. The individual Cy5 dyes' centers were found by curve fitting the image to a two-dimensional Gaussian, $f(x,y)=z_0+A*\exp(-0.5[((x-\mu_x)/\sigma_x)^2+((y-\mu_y)/\sigma_y)^2])$[45,75,76]. Calculation of the mean distribution with a minimized standard error allowed the determination of one Cy5 dye position before and after one step with nanometer resolution.

A sample Cy5 single fluorophore localization (SFL) is shown in Figure 47. This point spread function (PSF) was collected with the Andor iXon DV887 camera after a 0.5 s on-chip integration time, and it fit well to the two-dimensional Gaussian function (r^2=0.9514, X^2= 1.14) with a σ_μ = 0.19 nm.

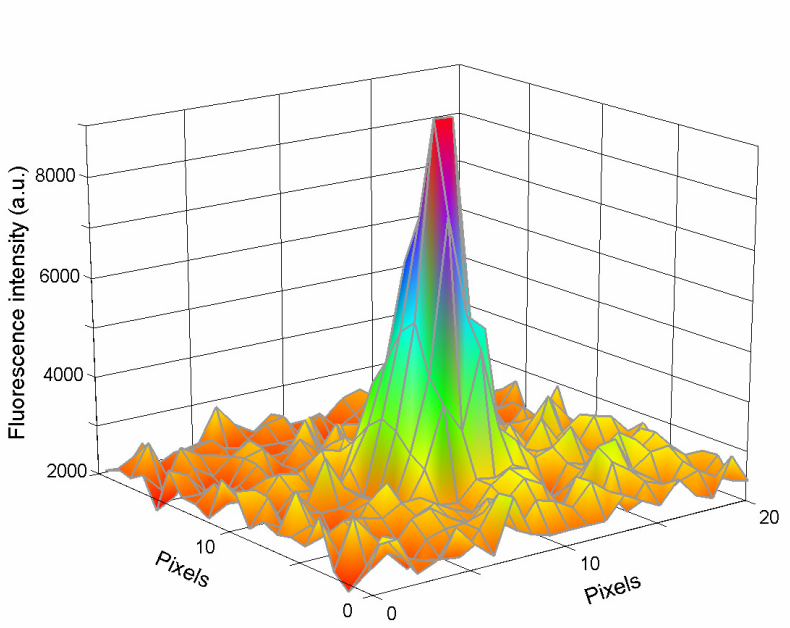

Figure 47: Example of a two-dimensional Gaussian curve fit to the PSF of a single Cy5 fluorophore (1 pixel = 74.3 nm).

To allow imaging of a single myosin VI at the same position for multiple frames the ATP concentration was lowered to 3 µM. The example fluorophore in Figure 47 was imaged for 20 frames with each 0.5 s exposure time. The fluorescence of the Cy5 spot dropped to background in a single step, suggesting that it either photobleached or the motor detached after this time. Localization of the PSF in each frame resulted in a standard deviation of 6.5 nm. A large component of the localization variance is likely due to the flexibility of the actin filaments bridging the beads: the actin filaments are only secured when they are in contact with a bead; hence, the stretch of filament between beads is loose enough to undergo Brownian motion.

To further demonstrate that the setup can accurately measure step sizes of a single motor, the nanometric piezostage was moved in user-defined increments. Myosin VI molecules bound to actin filaments in rigor lead to immobilized Cy5 fluorophores on the cover slip in the absence of ATP. Using these cover slips, 72 nm stage movements were simulated. The mean of the Gaussian distribution of discrete Cy5 fluorophore displacements was determined to be ~72 nm (Figure 48).

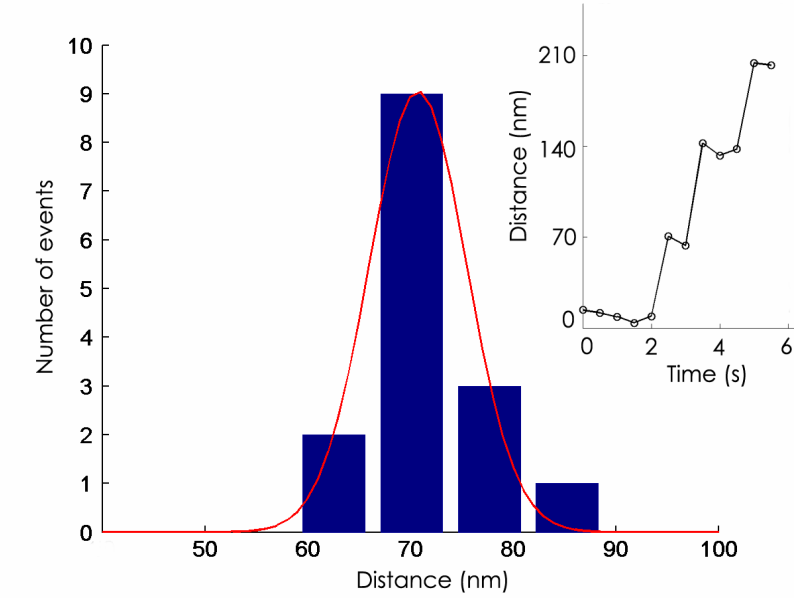

Figure 48: Histogram of the piezostage stepping with a mean distribution of 71 nm. The inset shows an example trace for the nanometric piezostage movement in defined increments of 72 nm.

Myosin VI takes ~72 nm Steps on Actin

As the Cy5 labeled myosin VI moves along the actin in the presence of 40 µM ATP, displacements of the Cy5 fluorophore occurring in discrete steps can be seen. Three example traces are shown in Figure 49.

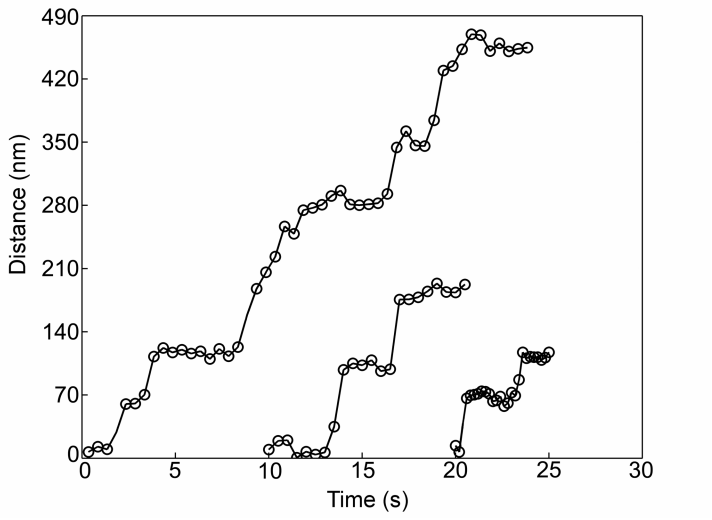

Figure 49: Stair cases of three different fluorescently labeled myosin VI molecules. These stair cases visualize the processive stepping of myosin VI on actin filaments. The integration time is 0.5 s for all stair cases. The ATP concentration was 40 µM.

85 transitions of 67 individual single fluorescently labeled myosin VI heads were analyzed under zero load conditions. The mean of the step size distribution was found to be 70 ± 23 nm (Figure 50). The second peak of 165 ± 15 nm on the histogram presumably represents two rapid steps that could not be resolved.

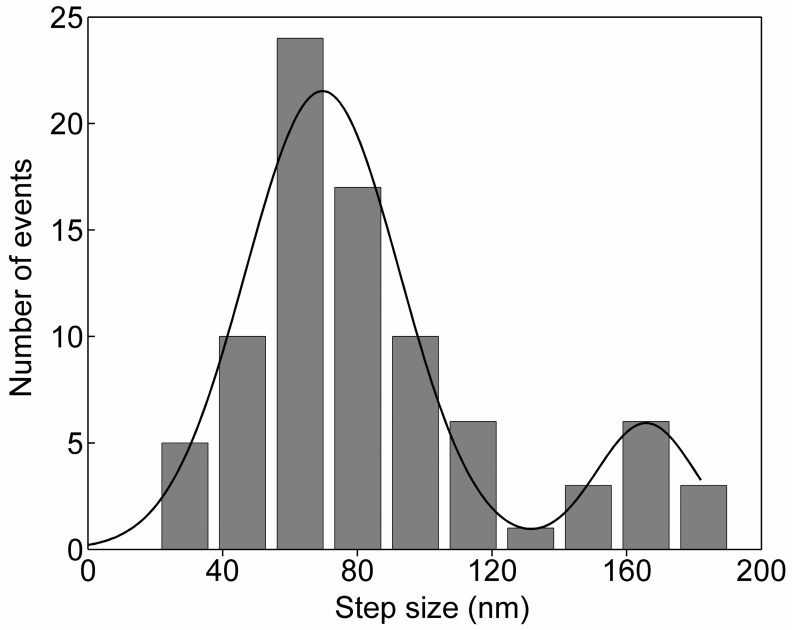

Figure 50: Step size histogram of single fluorescently labeled myosin VI molecules. The data is fit to a double Gaussian with a mean step size distribution of 70 ± 23 nm for the main peak and 165 ± 15 nm for the second peak. The second peak presumably represents two rapid steps that could not be resolved.

For the step size histogram, only motors that were close to the surface of the evanescent field yielded high enough numbers of photons to localize with high resolution. Molecules close to the surface have decreased processivity, and therefore most of the steps came from single transitions of myosin VI. Under low loads, myosin VI steps ~36 nm in optical trapping assays[49,74], which is half of the fluorophore displacement size determined in the present experiment. The 72 nm displacement of the fluorophore strongly supports a hand-over-hand mechanism and the use of a mechanically extensible element in the tail domain to extend the reach of the lever arm[66] (Figure 39). The results are not consistent with a mechanically extensible element N-terminal to the calmodulin binding site (Figure 40) or an inchworm model (Figure 41).

Stepping Mechanism of Myosin VI

In optical trapping experiments myosin VI displayed an unexpectedly big step size and a broad step size distribution, respectively[35]. The existence of mechanically extensible elements (such as the unique insert) was proposed to explain the unusual stepping behavior of myosin VI[35]. In this present work, the observed 72 nm displacement of one head during one ATPase cycle provides strong evidence for the existence of a mechanically extensible element which would have to derive from the tail domain[66]. The proximal tail domain (first ~80 residues following the IQ domain) is proposed to provide the flexibility because this domain is predicted to have a low propensity to form a coiled-coil[50,74]. In EM and single molecule studies, Rock *et al.* demonstrated subsequent to this work that the proximal tail domain is indeed the flexible element responsible for the large step size of myosin VI[77].

More importantly, this work provides strong evidence for a hand-over-hand stepping mechanism of myosin VI because the displacement of one head is twice the step size measured in optical trapping experiments[35]. These results show that myosin VI does not utilize a fundamentally different stepping mechanism than other characterized myosins in the myosin superfamily. The stepping mechanism of myosin V and myosin VI seems to differ primarily in their different partial contributions of the power stroke and the diffusive search to the step size. Myosin V stepping is determined largely by a power stroke with a smaller contribution of a diffusive search that leads to a narrow step size distribution[34,78]. Myosin VI stepping on the other hand is largely determined by a diffusive search deriving from the proximal tail domain that leads to a broad step size distribution. The power stroke, recently measured to be ~12 - 18 nm[51,75] presumably biases the leading head and determines the direction of movement.